COMMUNICATIONS IN
DEVELOPMENT AND ASSEMBLING OF TEXTILE PRODUCTS

Development of geodesic warp lines on point clouds for knitting graph calculation

Franz Dietrich[1]*, Daria Dordina[2], Daniel Lordick[2], Pulkit Mishra[1]
[1]*Textilforschungsinstitut Thüringen Vogtland e.V., Greiz, Germany*
[2]*Institut für Geometrie (GMV), TU Dresden, Dresden, Germany*
*Corresponding author

INFO

CDATP, ISSN 2701-939X
Peer reviewed article
2025, Vol. 6, No. 1, pp. 47-54
DOI 10.25367/cdatp.2025.6.p47-54
Received: 17 April 2024
Accepted: 04 January 2025
Available online: 13 July 2025

ABSTRACT

Flat knit has a high potential for networked production, but is also well suited for various smart textile applications and the single-piece production of close-to-skin (CTS) textiles with a high level of technology integration. Despite this good starting point, there are still major gaps in digital engineering that is based on 3D CAD development environments. Within future production platforms for customizable flat knit products, digital design and data for manufacturing, simulation, and visualization data are indispensable prerequisites. Appropriate procedures and algorithms are the subject of current international research. This paper contributes a new point-cloud-based approach for the digital creation of knitting charts and the graphic representations of knitted fabric suitable for production on knitting machines for CTS knitwear. Knitting charts, the mesh-loop representations (e.g., bitmaps) of discrete geometric developments of knittable polygon meshes, are derived from hybrid graph-based 3D abstractions. Another focus is efficient data handling, which is a fundamental step in achieving end-to-end process digitization for personalized smart textiles and wearables, including sensor-integrated workwear or medical devices.

Keywords
flat knit,
close-to-skin (CTS) textiles,
knitting warp lines,
reverse engineering,
knitting graphs,
point cloud data

1 Introduction

Major companies in the medical technology industry and their customers have long benefited from the advantages of digitally semi-customizable supports, for example medical orthoses and knee bandages, using the flat knitting process. The use of 3D CAD data obtained from 3D scans, combined with advanced optimization algorithms, has the potential to further streamline these processes and achieve an optimized and vivid fit in the future. Body parts distinguished by high concave and convex plasticity, such as the back of the knee, crook of the arm and kneecaps, gain significant advantage from the inclusion of scan data and the semi-automated reverse engineering or digital product development. CAD processes offer the advantage of reducing the time required to create knitting charts (KC) and increase precision in product development. They also enable rapid prototyping in three-dimensional flat knitting. The calculation of knitting graphs (KG), a preparatory step required for KC, is essentially based on Warp-Lines as proposed by Popescu et al. [1], which are constructed in the warp direction using various methods, for example, building geodesics. As mentioned by Dietrich and Kyosev, methods of differential calculus, such as the heat method or the scalar field method, can play a decisive role in the generation of these geodesics [2]. Current descriptions of the methods include the auxiliary use of meshes or NURBS surfaces. The work presented here demonstrates a novel method that constructs warp lines, directly based on a point cloud. This technique allows the work with desired local neighborhood size. Point clouds are estimated using various criteria, including local curvature value, distance between points, geodesic curve smoothness, etc. The proposed method enables precise and controllable parametrization of complex scanned shape. This innovative approach sets itself apart from existing methods and signifies potential advancements in the field of digital knitting data computation.

Relating this context, point clouds offer a few advantages over NURBS or meshes. Depending on the scanning system used, point clouds demonstrate a higher degree of precision, as they do not require conversion or interpolation like NURBS or meshes. This absence of intermediary steps leads to a more accurate representation.

The production of close-to-skin garments requires a precise representation of body shapes, with data initially obtained through 3D-scanning techniques. Traditionally, the transition from discrete point cloud data to continuous geometry has been facilitated through meshing processes. For example, the mesh geometry for knitting purposes is further processed by calculating a Reeb graph and a monotonic time function as proposed by Narayanan [3] or, as suggested by Popescu et al., by contouring the input geometry and then transversely recalculating the weft and warp lines [1].

However, the meshing process of point clouds usually involves the interpolation of data points using algorithms such as Poisson Surface Reconstruction or Marching Cubes. The inherent scale variability within the body geometry can lead to loss of detail in certain regions, which affects the accuracy of the final representation. Furthermore, in terms of data storage, it would be more advantageous to work directly with the point cloud data.

In contrast to larger-scale scans, such as terrain or architectural-scale scans, which often suffer from artifacts and uneven point distribution, body part scan data exhibit higher uniformity and completeness, enabling accurate representation of geometric features. Leveraging this advantage and employing techniques rooted in geometric analysis and eigenvalue computation [4], it is possible to identify and extract crucial structural and shape features from the scan data [5]. Computed values can be converted into scalar fields and written as data into the point clouds. For instance, in the ASCI color fields R, G, B can be overwritten to different scalar fields. The use of several fields allows the representation of input geometry features on various scales or according to various requirements, such as flat regions or regions with high curvature. Therefore, these important features can be considered during the KG calculation.

As indicated above, various methods for KG construction are currently being developed or refined. Each of the current methods has area-specific advantages and disadvantages. In particular, the influence of various conditions or restrictions on the KG calculation is becoming increasingly important. On the one hand, the influence serves a more precise control of algorithmic artifacts and, on the other hand, a higher influence regarding machine-compatible data generation (knitting time, line errors, mesh formation techniques) [1,2,6-9].

2 Methods

The full process of creating the knitting chart is described in the flow chart below (Fig. 1). However, the article only deals with the first computational steps from point cloud processing to the KG computation and does not consider further steps of the KC calculation.

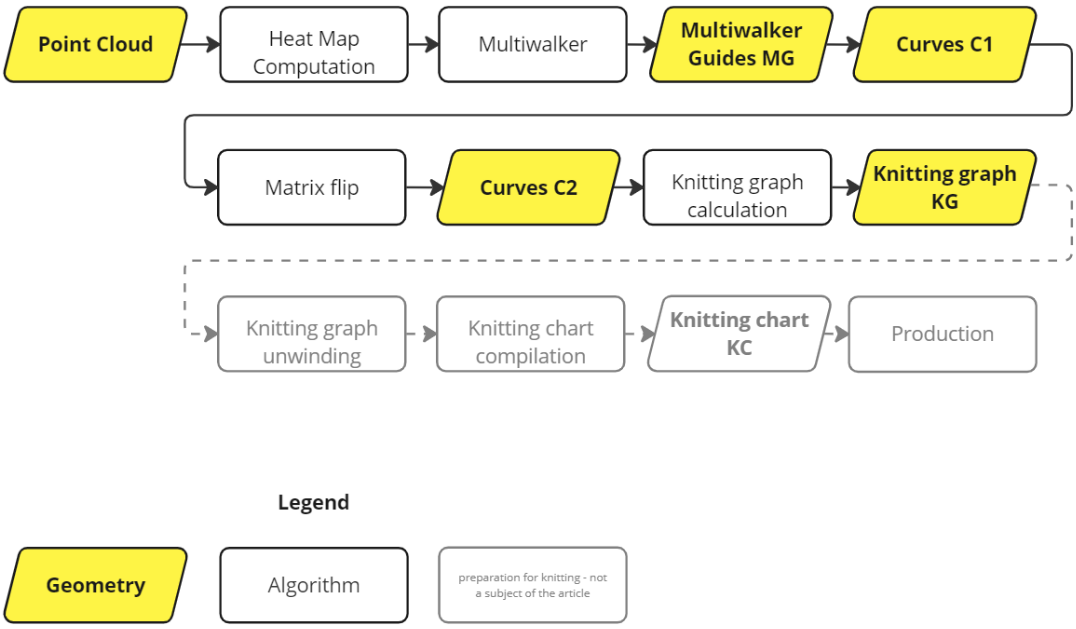

Fig. 1 Flow chart of process chain.

2.1 Heat Method

The heat method originally presented by Keenan Crane in 2013 is used to derive geodesics. In this technique, heat is allowed to diffuse briefly across a discrete 3D geometry (e.g. a mesh or point cloud). The temperature gradient is then normalized and inverted to obtain a unit vector field to which the geodesics are aligned. In practical applications, performance is typically an order of magnitude faster than modern methods while maintaining comparable accuracy [11]. This method can be applied in any dimension and on any domain that admits a gradient and an inner product, including regular grids, triangular meshes, and point clouds. For this study, Nicholas Sharp's implementation, "Point Cloud Distance & Vector Heat" [12], was used as a Python script in Rhinoceros 3D. The script allows the input of one or more heat sources. To calculate the geodesics for a shape (here: scan of a leg segment), only one heat source was entered at the lower end. This means that the heat is distributed almost linearly over the shape. The heat map is created in RGB colors over the point cloud (Fig. 2a). The following section describes the building of geodesics for knitting path calculation using the multiwalker method. The point cloud with the inscribed RGB information is used as the most important weighting parameter.

2.2 Multiwalker

The algorithm published by Dordina et al. (2023) aims to navigate through a point cloud from one point to another, where the selection of points is determined by geometric criteria. Technically, the algorithm can be applied to different types of geometry.

In the case study of a medical knee bandage, the shape is complex and free-form, but primarily exhibits a cylinder-like shape with upper and lower boundaries. The inputs for the algorithm include a point cloud with pre-computed scalar fields inscribed as floating-point color properties, a set of starting points on the top boundary, and a corresponding set of end points on the bottom boundary. The only adjustable parameter available to the user is the number of neighboring points (N).

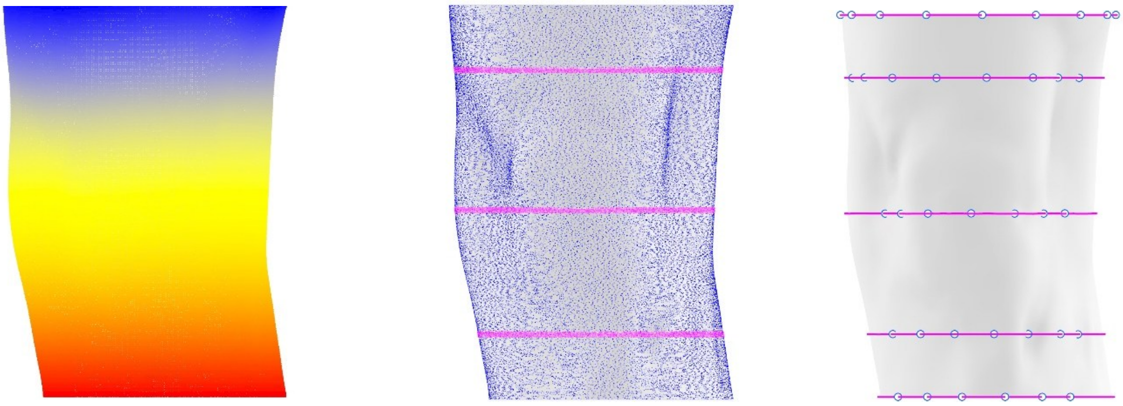

Fig. 2 (a) heat map on point cloud; (b) calculated PC intersection; (c) interpolated curve with SPs.

Initially, we compute an R-Tree for the entire point cloud. For each starting point, we evaluate and compare N surrounding points using different criteria such as scalar field values, distance between points, smoothness criteria, etc. The values for each point are then aggregated, and based on this final score, the next point in the sequence is selected. The computation runs in parallel. This algorithm enables us to accurately estimate the complex deformed shape. The outcome of the algorithm is a collection of ordered point sequences that traverse the point cloud geometry. Each point sequence characterizes a principal curve, which serves as the foundation for subsequent KG calculations.

2.3 Multiwalker Warp Building

The colored point cloud is used as input for the multiwalker method. In addition, n point cloud sections were calculated through the intersection of n xy planar planes and the PC (Fig. 2b). A curve is interpolated through each of the intersections and then divided into a number i of points. Whereby the curve length l by i calculates the distance of the points dp (1) to each other (Fig. 2c). The resulting lists of points form the source points (SP).

$$dp = \frac{l}{i} \tag{1}$$

These SP lists with a uniform number of points are used to be crossed by the multiwalker. Each point at the same index is used as a necessary crossing point. The point on the first [0] and last path [-1] (list-index) forms the start and end point. The points derived by the intersection between [0] and [-1] form the guide points P_{ij} (2). The multi-walker warp lines are formed by using the start, guide and end points with the same index to calculate the multiwalker route through the point cloud. The guide points stabilize the course, especially in the case of strong geometric bends such as the bent knee.

$$P_{ij} = P_{0j} . \frac{i}{n-1} . (P - 1j - P_{0j}) \tag{2}$$

The calculated Multiwalker Warps (MWW) (Fig. 3a) have specific continuities depending on the point cloud density and the given neighborhood size. Depending on the accuracy requirements, the final MWWs can also be derived by first interpolating the source points with a curve and then recalculating the curve with a lower number of points, whereby the number of points can be influenced by a tolerance value.

As defined by M. Poposcu, a weft fabric can be described in simplified terms as follows: a row of stitches in the width is called a stitch row and represents the weft direction, while a column of loops in the length represents the warp direction [3]. For the calculation of the knittable graphs described in the following section, the curves in the warp line direction are required as a basis. For this purpose, all the calculated MWW are reworked. All MWW are subdivided into an equal number of points. The matrix of points is then flipped. The flipped matrix is used to calculate the closed curves C1 (Fig. 3b). After dividing C1 into equally distanced points (CP1), the matrix is flipped again and the final warp lines (C2) lines are rebuilt transverse (Fig. 3c). The distance between the points CP1 should ideally correspond to the stitch width. However, the current implementation only allows an approximation of this distance by dividing the C1.

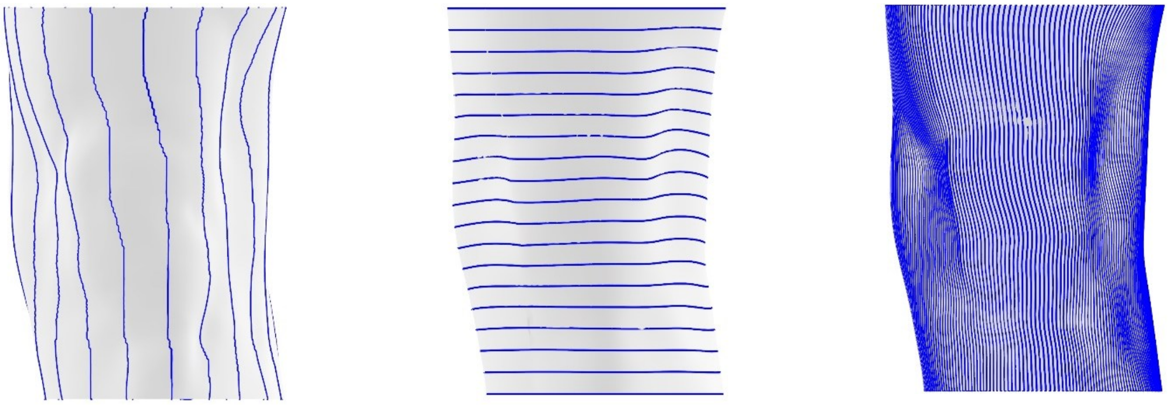

Fig. 3 (a) MWW lines; (b) flipped matrix C1 curves; (c) flipped matrix C2 final warp lines.

2.4 Hybrid Graph Method

In the publication by Dietrich and Kyosev (2023), mentioned in the introduction, a possible method for calculating the KG (Fig. 4a), aka. hybrid graph, is presented [2]. The method described above and the hybrid graph method proposed by Dietrich and Kyosev show similarities regarding the creation of weft lines, although the generation of the necessary warp lines is different and appears to be solvable in many ways. We would tend to use the general term hybrid graph methods (HGM) here. Here in brief is the generation of the KG based on the MWW described above.

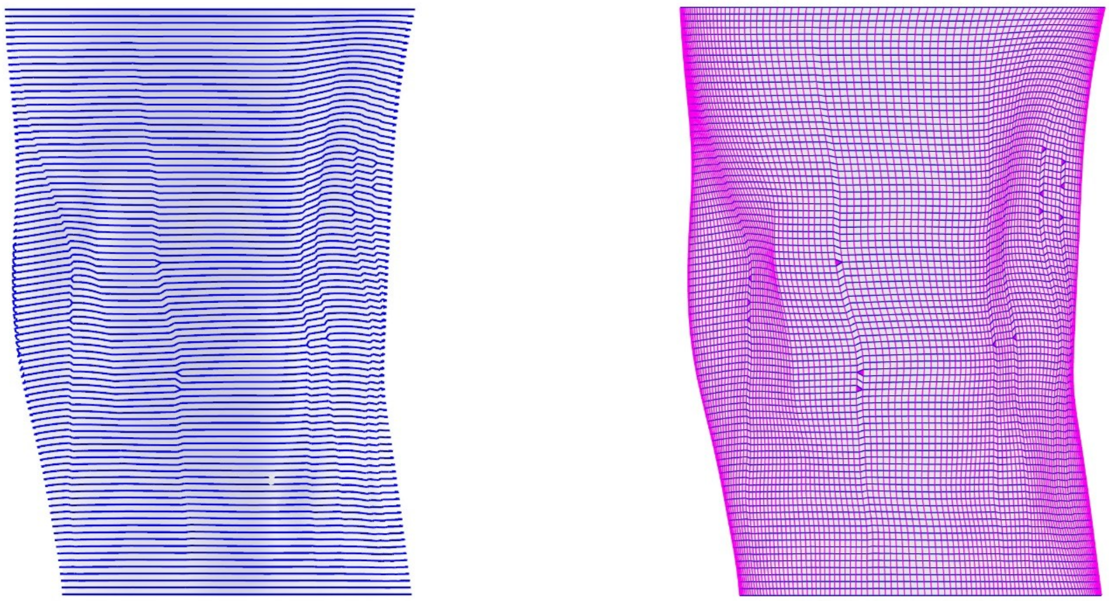

Fig. 4 (a) calculated knitting graph (KG); (b) knitmesh

After constructing all MWW, they are processed pairwise in a loop. The entire list is partitioned pairwise, with each iteration processing $i + 1$. Both curve lengths GL_i are divided by a divisor d, which corresponds to the the stitch height. This division determines the point spacing on the warp lines curves. This means that for each pair of warp lines $(G_{i,} G_{(i+1)})$ a set of points P is defined, where each point P_j in G_i and $G_{(i+1)}$ is calculated by the formula

$$P_{j0} = \frac{GL_i}{d} \text{ and } P_{j1} = \frac{GL_{i+1}}{d}. \tag{3}$$

The resulting graph matrix is then iterated in another function with the following condition. Each point on the lower of the paired curves searches for the two nearest points on the second curve. The distances are measured, and the point with the shortest distance from the starting point is used to create a line.

This process runs sequentially through each pairwise row and then moves on to the next one. This sequential approach reduces parallel computations during a loop and stabilizes the graph construction. These points $P_{i,j}$ and $P_{i+1,k}$ are then connected to generate the KG.

2.5 Knitmeshes

Fig. 3c shows the rebuild C2 curves (C2C) in warp direction. Fig. 4a and 5a show the calculated KG based on the C2C. A knitmesh (KM) was derived which can be used to create the KC. Another possible use of the KM is a quantitative evaluation of the distance deviation between the point cloud and the KM. KM are formed from the sorted line segments of the KG. Fig. 4b and 5b show the superimposed C2C (warp lines) and the calculated KG. The sorting of the blue KG segments (KGS) is based on one of the paired C2Cs. All KGS are assigned to their starting points according to one of the C2Cs. The starting point must form an intersection with an C2C. The KGS are then sorted within the C2C domain and vertices are derived for the KM construction.

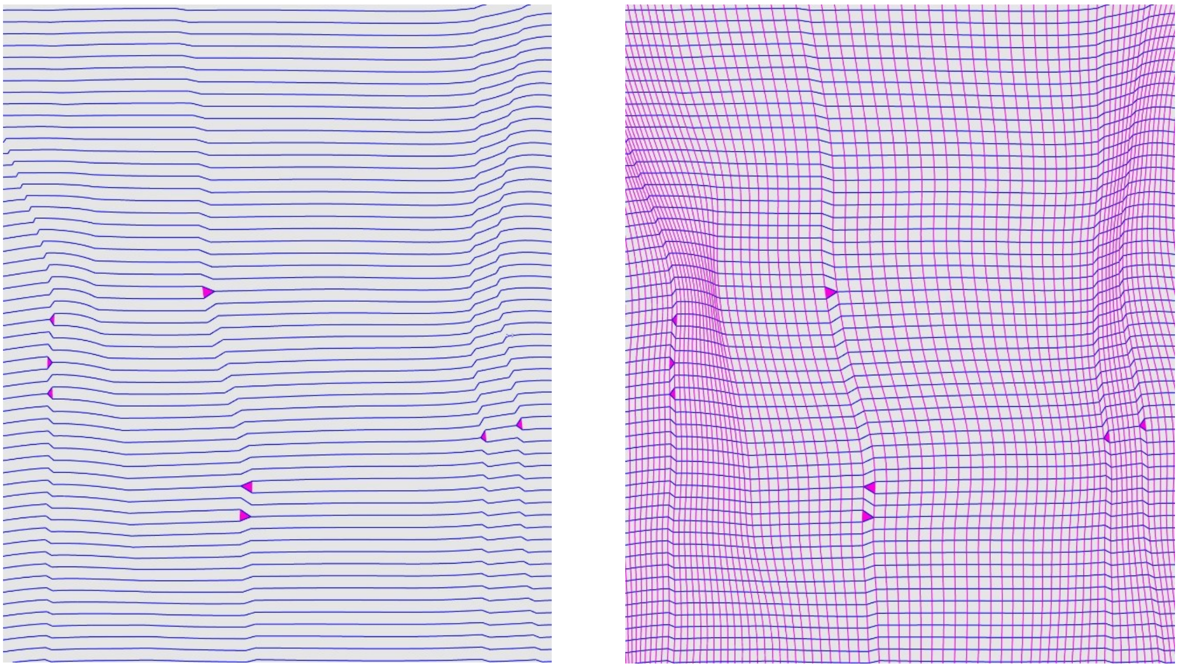

Fig. 5 (a) final KG; (b) knitmesh with in- and decrease mark triangle.

3 Conclusions

The physical results currently depend on the knitting samples, which are still under development. The digital KG calculations from the MWW-approach, proposed here, shows a good qualitative correlation with the HGM-approach based on polygon mesh models. However, the differences between the HGM on polygon meshes and the HGM on pure point clouds proposed here and the knitting quality of the KG is generally very dependent on the calculated topology and point cloud density. This should be investigated in more detail in subsequent studies. In the present study, a distance analysis of the KM (Fig. 5. c) to the input point cloud is calculated and the standard deviation is used as a comparative feature.

The KG (Fig. 3b) probably show no strong formation of short rows or frequent increase and decrease due to the relatively low curvature of the input point cloud. For better visibility, increases and decreases at the end of a short row are marked with triangles (Fig. 5b). A deviation analysis between KM and the point cloud shows a standard deviation of 0.29562 mm. This means that the calculated KM and the derivable graph are just within the measurement accuracy (0.1-0.3 mm) of the ARTEC EVA handheld scanner. A measurement noise of up to a further 0.3 mm due to various measurement inaccuracies and motion blurring can be assumed. A more precise determination of the accuracy is only possible with a statically calibrated system.

In conclusion, the proposed methodology offers a significant advantage through its efficient data handling capabilities and contribution to process digitization, which are crucial for enhancing productivity and quality within manufacturing. The algorithms described above enable precise manipulation of scanned data from various body parts. However, the utilization of point clouds as input data is contingent upon the calculated topology and density of said point clouds, implying potential challenges in attaining consistent outcomes across diverse scenarios.

The primary application of the proposed methodology lies in its implementation for customizable flat knit products. It holds promise for the singular production of tailored close-to-skin (CTS) textiles and potentially smart textile applications.

Author Contributions

F. Dietrich: conceptualization, methodology, investigation,validation, formal analysis, Software, visualization, writing, creating the initial draft, writing – original draft preparation; D. Dordina: conceptualization, methodology, writing, creating the initial draft; investigation, validation, formal analysis, Software, writing – original draft preparation; D. Lordick: monitoring, writing – reviewing and editing, supervision, project administration; P. Mishra: creating the initial draft, monitoring, writing – reviewing and editing, project administration.

Acknowledgements

Special thanks go to Mr. Ibrahim Halvani from TITV Greiz (Textilforschungsinstitut Thüringen Vogtland e.V.) for the realization of the knitting specimen. He implemented the calculated KC in bitmap format from Rhinoceros 3D/Grasshopper. The KC were programmed with the STOLL M1 software and a STOLL ADF 530-32 ki-W multigauge flat knitting machine (i7.2, 1.82mm).

Conflicts of Interest

The authors declare no conflict of interest.

References

1. Popescu, M.; Rippmann, M.; van Mele, T.; Block, P. Automated Generation of Knit Patterns for Non-developable Surfaces. In *Humanizing Digital Reality*; De Rycke, K., et al., Ed.; Springer, Singapore, 2018. DOI: https://doi.org/10.1007/978-981-10-6611-5_24.
2. Dietrich, F.; Kyosev, Y. Adaptive building of truss network for deformation analysis of 3D-knitted technical-textiles. In *Proc. of International Conference – Smart Textiles and Emerging Technologies*, 1(1), 1-12. 2023. ISSN 3021-1239. DOI: https://doi.org/10.61135/stet2023.
3. Narayanan, V.; Albaugh, L.; Hodgins, J.; Coros, S.; McCann, J. Automatic Machine Knitting of 3D Meshes. *ACM Trans. Graph*. **2018**, *37*, 35. DOI: https://doi.org/10.1145/3186265.
4. Maćkiewicz, A.; Ratajczak, W. Principal components analysis (PCA). *Computers & Geosciences* **1993**, *19*, 303-342. DOI: https://doi.org/10.1016/0098-3004(93)90090-R.
5. Rodríguez-Gonzálvez, P.; Fernández-Palacios; B. J. Point cloud optimization based on 3D geometric features for architectural heritage modeling. *Disegnarecon* **2021**, *14*, 18. DOI: https://doi.org/10.20365/DISEGNARECON.26.2021.18.
6. Karmon, A.; Sterman, Y.; Shaked, T.; Sheffer, E.; Nir, S. KNITIT: a computational tool for design, simulation, and fabrication of multiple structured knits. In *Proc. of the 2nd Annual ACM Symposium on Computational Fabrication* 2018, 4. DOI: https://doi.org/10.1145/3213512.3213516.
7. Nader, G.; Quek, Y. H.; Chia, P. Z.; Weeger, O.; Yeung, S.-K. KnitKit: A flexible system for machine knitting of customizable textiles. In *ACM Transactions on Graphics (Siggraph 2021)*.
8. Mitra, R.; Makatura, L.; Whiting, E.; Chien, E. Helix-Free Stripes for Knit Graph Design. In *SIGGRAPH '23: ACM SIGGRAPH 2023 Conference Proceedings* 2023, 75. DOI: https://doi.org/10.1145/3588432.3591564.
9. Lin, J.; Narayanan, V.; Ikarashi, Y.; Ragan-Kelley, J.; Bernstein, G.; McCann, J. Semantics and Scheduling for Machine Knitting Compilers. *ACM Trans. Graph*. **2023**, *42*(4), 143.

10. Dordina, D.; Milkau, C.; Tošić, Z.; Lordick, D., Schneider, D. Point Cloud to True-to-Deformation Free-Form NURBS. In *Advances in Architectural Geometry*, Kathrin Dörfler, Jan Knippers, Achim Menges, Stefana Parascho, Helmut Pottmann and Thomas Wortmann, Ed.; Berlin, Boston: De Gruyter, 2023; 125-136. DOI: https://doi.org/10.1515/9783111162683-010.
11. Crane, K.; Weischedel, C.; Wardetzky, M. The Heat Method for Distance Computation. *ACM Transactions on Graphics* **2013**, *32*(5), 90-99. DOI: https://doi.org/10.1145/3131280.
12. Sharp, N. potpourri3d V1.0.0. https://github.com/nmwsharp/potpourri3d (accessed 2023-07-20).